MOLECULAR AND CELLULAR BIOLOGY, July 2004, p. 6456–6466 Vol. 24, No. 14
0270-7306/04/$08.00+0 DOI: 10.1128/MCB.24.14.6456–6466.2004

Insulin Increases Cell Surface GLUT4 Levels by Dose Dependently Discharging GLUT4 into a Cell Surface Recycling Pathway†

Roland Govers,[1]* Adelle C. F. Coster,[2] and David E. James[1]*

Diabetes and Obesity Research Program, Garvan Institute of Medical Research, Darlinghurst, Sydney, New South Wales 2010,[1] and School of Mathematics, University of New South Wales, Sydney, New South Wales 2052,[2] Australia

Received 3 March 2004/Returned for modification 8 April 2004/Accepted 27 April 2004

The insulin-responsive glucose transporter GLUT4 plays an essential role in glucose homeostasis. A novel assay was used to study GLUT4 trafficking in 3T3-L1 fibroblasts/preadipocytes and adipocytes. Whereas insulin stimulated GLUT4 translocation to the plasma membrane in both cell types, in nonstimulated fibroblasts GLUT4 readily cycled between endosomes and the plasma membrane, while this was not the case in adipocytes. This efficient retention in basal adipocytes was mediated in part by a C-terminal targeting motif in GLUT4. Insulin caused a sevenfold increase in the amount of GLUT4 molecules present in a trafficking cycle that included the plasma membrane. Strikingly, the magnitude of this increase correlated with the insulin dose, indicating that the insulin-induced appearance of GLUT4 at the plasma membrane cannot be explained solely by a kinetic change in the recycling of a fixed intracellular GLUT4 pool. These data are consistent with a model in which GLUT4 is present in a storage compartment, from where it is released in a graded or quantal manner upon insulin stimulation and in which released GLUT4 continuously cycles between intracellular compartments and the cell surface independently of the nonreleased pool.

There are at least 12 facilitative sugar transporters in mammals. Glucose transporter 4 (GLUT4) plays an important role in regulated glucose transport, as is observed in the postprandial state and during exercise. GLUT4 is highly expressed in cell types that exhibit regulated glucose uptake, such as adipocytes, skeletal muscle cells, and cardiomyocytes. The intracellular trafficking of GLUT4 is a major determinant of its acute regulation (4). In the basal nonstimulated state, GLUT4 is present in an intracellular tubulovesicular compartment, from which it undergoes insulin-dependent movement to the cell surface, resulting in a 10- to 20-fold increase in cell surface GLUT4 levels.

There are two major questions concerning the trafficking of GLUT4 in insulin-responsive cell types. What is the nature of the intracellular insulin-sensitive GLUT4 storage compartment, and how does insulin provoke the release of GLUT4 from this site to the cell surface? Two models that address these questions have been proposed. In the first, GLUT4 is targeted to a specialized (nonendosomal) secretory compartment that undergoes regulated exocytosis in response to insulin stimulation. The second suggests that GLUT4 is retained within endosomal or endosome-associated structures and that insulin overcomes this retention mechanism, releasing GLUT4 into recycling vesicles. In addition, adaptations of these models can be envisaged, while they also do not necessarily need to be exclusive.

In evaluating GLUT4 trafficking data, it is important to recognize the cell type under investigation. For example, many experiments have been conducted in CHO cells or 3T3-L1 fibroblasts, in which GLUT4 is not expressed endogenously. In these cell types, exogenous GLUT4 colocalizes with endosomal markers, such as the transferrin receptor, but recycles more slowly than the transferrin receptor and undergoes modest insulin-dependent movement to the cell surface (10, 11). In contrast, in bona fide insulin target cells such as muscle cells and adipocytes, a significant portion of intracellular GLUT4 (≈50%) is excluded from endosomes (15, 35). Because the magnitude of the insulin response in these cells tends to be larger than CHO cells and 3T3-L1 fibroblasts, this nonendosomal compartment may represent a specialized secretory pool.

An alternative view is that the nonendosomal GLUT4 pool is represented by the trans-Golgi network (TGN) and vesicles that recycle between endosomes and the TGN. Several observations point to a role for the TGN in GLUT4 trafficking. Morphological studies show that a significant proportion of GLUT4 is clustered in the TGN area (22, 29). The TGN adaptor protein AP-1 associates with GLUT4-containing vesicles in vivo and in vitro (7, 18). Other proteins that localize to the TGN or recycle between endosomes and the TGN are enriched in GLUT4-containing membranes, including the cation-dependent mannose 6-phosphate receptor, syntaxin 6, and syntaxin 16 (23, 28). In addition, the insulin-responsive aminopeptidase, whose trafficking closely resembles that of GLUT4, traverses the TGN after internalization from the plasma membrane (PM) as measured by resialylation after neuraminidase treatment (28). Intriguingly, there is very little overlap between GLUT4 and the TGN marker TGN38 (19, 28), indicating that

* Corresponding author. Present address for Roland Govers: Department of Functional Genomics, Center for Neurogenomics and Cognitive Research, Free University and Free University Medical Center, WN Building, Rm. A445, De Boelelaan 1087, 1081 HV Amsterdam, The Netherlands. Phone: 31-20-4446929. Fax: 31-20-4446926. E-mail: roland@cncr.vu.nl. Mailing address for David E. James: Diabetes and Obesity Research Program, Garvan Institute of Medical Research, 304 Victoria St., Darlinghurst, Sydney, New South Wales 2010, Australia. Phone: 61-2-9295810. Fax: 61-2-92958201. E-mail: d.james@garva.org.au.

† Supplemental material for this article may be found at http://mcb.asm.org/.

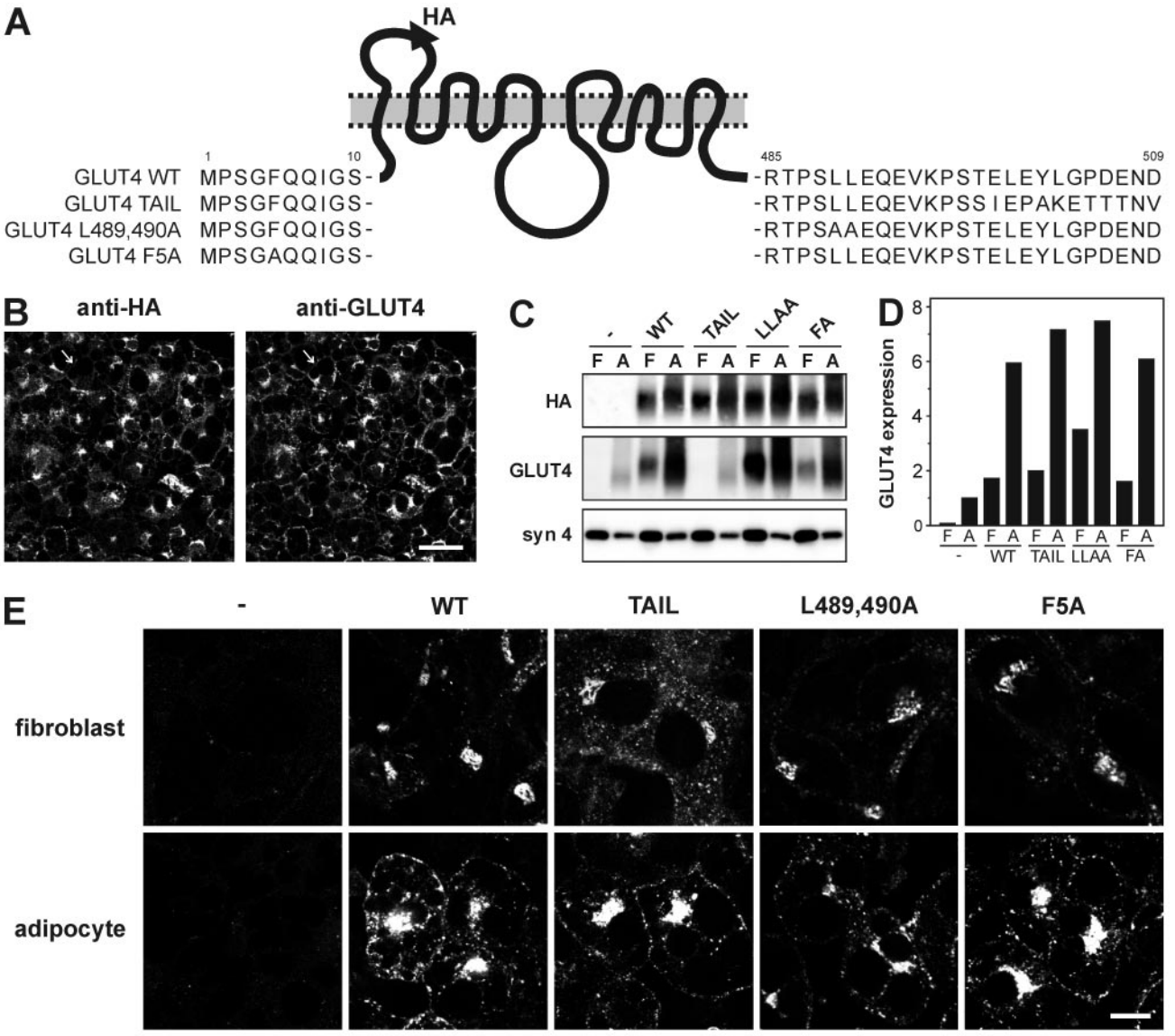

FIG. 1. Characterization of GLUT4 mutants. (A) Schematic representation of HA-tagged wild-type GLUT4 (WT), GLUT4 Tail mutant, GLUT4 L489,490A, and GLUT4 F5A. (B) 3T3-L1 adipocytes expressing HA-tagged wild-type GLUT4 were immunolabeled with anti-HA and anti-GLUT4 for the detection of HA-GLUT4 and total cellular GLUT4 content, respectively. Arrow indicates a cell that does not express HA-GLUT4. Bar, 30 μm. (C) 3T3-L1 fibroblasts (F) and 3T3-L1 adipocytes (A) expressing the indicated HA-tagged GLUT4 molecules were lysed, and equal amounts of protein were analyzed by Western blotting with the indicated antibodies. The syntaxin 4 immunoblot serves as an internal control. (D) The blots in C were analyzed as described in Materials and Methods, and GLUT4 overexpression was compared to endogenous GLUT4 expression in noninfected adipocytes. The anti-HA immunoblot was used to determine the relative expression of GLUT Tail, as this molecule is not recognized by the anti-GLUT4 antibody. (E) Nonstimulated 3T3-L1 fibroblasts and adipocytes expressing the indicated HA-GLUT4 molecules were immunolabeled with anti-HA. Bar, 10 μm.

GLUT4 may be localized to a subcompartment of the TGN. Such a trafficking pathway could result in enhanced insulin responsiveness indirectly by sequestering GLUT4 in the absence of insulin.

In the present study, we examined various aspects of GLUT4 trafficking in 3T3-L1 fibroblasts/preadipocytes and adipocytes with a novel technique that allows kinetic and quantitative analysis. These studies show that the intracellular sequestration of GLUT4 in adipocytes is regulated by two mechanisms involving retention in endosomes and an intracellular cycle between endosomes and a nonendosomal compartment. We studied a GLUT4 mutant that does not enter the intracellular cycle in adipocytes as well as 3T3-L1 fibroblasts, in which GLUT4 is only retained in endosomes. In these cases, under basal conditions, we found higher levels of GLUT4 in the plasma membrane recycling pathway compared with wild-type GLUT4 in adipocytes. Nevertheless, there was a robust insulin responsiveness. These observations point to an important role for endosomes in insulin action. Moreover, insulin induces the release of GLUT4 into the cell surface recycling system in a

graded insulin dose-dependent manner, providing new insights into the nature of insulin action.

MATERIALS AND METHODS

Materials. 3T3-L1 murine fibroblasts were obtained from the American Type Culture Collection, Rockville, Md. Newborn calf serum and Dulbecco's modified Eagle's medium (DMEM) were from Invitrogen (Carlsbad, Calif.), fetal bovine serum was from Trace Scientific (Melbourne, Australia), insulin was from Calbiochem (San Diego, Calif.), and 3-isobutyl-1-methylxanthine, biotin, dexamethasone, and murine immunoglobulin G1-κ MOPC21 antibody from Sigma (St. Louis, Mo.). Normal swine serum was obtained from Dako Corporation (Carpinteria, Calif.). Anti-GLUT4 antibody, raised against its 12 C-terminal residues, and anti-syntaxin 4 antibody have been described previously (20, 27, 28). Monoclonal anti-HA antibody was obtained from Covance (Berkeley, Calif.), and fluorescent antibodies were from Molecular Probes (Leiden, The Netherlands). pCIS2/HA-GLUT4 plasmid was kindly provided by Michael Quon (21).

Cell culture. 3T3-L1 fibroblasts up to passage 20 were cultured in high-glucose DMEM supplemented with 10% heat-inactivated newborn calf serum at 37°C in 5% CO_2. For differentiation into adipocytes, fibroblasts were cultured in DMEM with newborn calf serum for 1 or 2 days postconfluence, after which the cells were cultured for 3 days in DMEM containing 10% heat-inactivated fetal bovine serum, 350 nM insulin, 0.5 mM 3-isobutyl-1-methylxanthine, 250 nM dexamethasone, and 400 nM biotin and for 3 days in DMEM containing 10% fetal bovine serum and 350 nM insulin. After differentiation, adipocytes were maintained in DMEM supplemented with 10% fetal bovine serum. Adipocytes were used for experiments 8 to 11 days after the onset of differentiation, and the medium was renewed 2 or 3 days prior to each experiment. For culturing in black clear-bottom gelatin-coated 96-well plates, cells were seeded at a 1:1 cell surface ratio, and differentiation was initiated 4 days postseeding. To express hemagglutinin (HA)-GLUT4 in fibroblasts and adipocytes, fibroblasts were infected with retrovirus as described previously (28) and differentiated into adipocytes as described above.

Fluorescence assays. Cells were grown in black clear-bottom 96-well plates as described above and starved for 2 h in serum-free DMEM supplemented with 0.2% bovine serum albumin before starting the experiment. Cells were maintained in serum- and bicarbonate-free DMEM containing 20 mM HEPES (pH 7.4) and 0.2% bovine serum albumin throughout the experiments. Experiments were performed in a 37°C water bath. All postfixation incubations were performed at room temperature. Four wells within a 96-well plate were used for every measurement. Within each experiment, two plates were incubated identically, and every experiment was performed at least twice (ranging from two to five times), resulting in at least four analyses per study. There was little variation between experiments. Representative experiments are shown. Error bars indicate standard deviations.

Translocation assay. Insulin was added at different time points, after which the cells were fixed for 15 min on ice and for 15 min at room temperature in 3% formaldehyde. After quenching for 5 min with 50 mM glycine, cells were incubated for 20 min with 5% normal swine serum in the absence or presence of 0.1% saponin to analyze the amount of GLUT4 at the PM or the total cellular GLUT4 content, respectively. Cells were incubated for 60 min with a saturating concentration of either an antibody directed against the HA tag (mouse immunoglobulin G1-κ subtype, 25 μg/ml) or a control nonrelevant antibody (mouse immunoglobulin G1-κ MOPC21; 25 μg/ml) in phosphate-buffered saline containing 2% normal swine serum. After extensive washing, the cells were incubated for 20 min with 5% normal swine serum in the presence or absence of 0.1% saponin to permeabilize all cells so that the background labeling of the secondary antibody was similar for all wells. Cells were incubated for 60 min with saturating concentrations of Alexa 488-conjugated goat anti-mouse antibody (20 μg/ml) and Alexa 594-conjugated wheat germ agglutinin (10 μg/ml) in phosphate-buffered saline containing 2% normal swine serum. After washing, fluorescence (emm 485 nm/exc 520 nm and emm 544 nm/exc 630 nm) was measured with the bottom-reading mode in a fluorescence microtiter plate reader (FLUOstar Galaxy; BMG Labtechnologies, Offenburg, Germany). The percentage of GLUT4 at the PM was calculated for each condition. Alexa 594-wheat germ agglutinin fluorescence was used to correct for variation in cell density in each well.

Internalization assay. For single-cycle internalization experiments, cells were stimulated for 20 min with 200 nM insulin after starvation and washed on ice with ice-cold DMEM containing 20 mM HEPES (pH 7.4) and 0.2% bovine serum albumin. Cells were incubated with 100 nM wortmannin or 200 nM insulin and either anti-HA (25 μg/ml) or nonrelevant antibody (MOPC21) in DMEM-HEPES-bovine serum albumin for 1 h on ice. Wortmannin was added to abolish insulin signaling. This drug has no direct effect on GLUT4 internalization in adipocytes (16) and has previously been used to study GLUT4 internalization (1, 33). Cells were washed extensively, after which either 100 nM wortmannin or 200 nM insulin in DMEM-HEPES-bovine serum albumin was added. The plate was then transferred to 37°C, and at different times, formaldehyde was added to the wells to a concentration of 3%. After 5 min, the formaldehyde was quenched. The cells were incubated for 20 min with 5% normal swine serum in the absence of saponin, labeled with Alexa 488-conjugated goat anti-mouse antibody and Alexa 594-conjugated wheat germ agglutinin, washed, and analyzed as described above.

Recycling assay. For continuous antibody uptake experiments, cells were incubated for 20 min with or without 200 nM insulin, after which anti-HA or nonrelevant antibody was added (50 μg/ml). The incubation was continued in the presence or absence of insulin for various time periods. Cells that were used to determine the total amount of HA-GLUT4 were not incubated with antibody during this 37°C incubation. After incubation, the cells were fixed and quenched as described above and incubated for 20 min with 5% normal swine serum and 0.1% saponin. Cells that were used to determine the total cellular amount of HA-GLUT4 were incubated for 60 min with anti-HA antibody or control antibody in phosphate-buffered saline containing 2% normal swine serum. All other cells were incubated with 2% normal swine serum without antibody. Subsequently, the cells were incubated with Alexa 488-conjugated goat anti-mouse antibody and Alexa 594-conjugated wheat germ agglutinin, washed, and analyzed. The amount of specific anti-HA uptake was expressed as a percentage of total cellular immunoreactive HA-GLUT4. Note that the increase in label at early time points represents binding of antibody to GLUT4 molecules that are already present at the PM as well as binding to GLUT4 molecules that become incorporated in the PM after the addition of antibody. Therefore, the initial increases in fluorescence do not represent initial GLUT4 trafficking rates. Due to the limited number of conditions that could be analyzed on a single 96-well plate, the 6-h time points of the recycling studies in which different insulin concentrations were tested are derived from distinct experiments (see Fig. 7).

Immunofluorescence microscopy. Cells were immunolabeled essentially as described above. For visualization of fat droplets, 1 μg of Nile red per ml was added during the secondary antibody incubation. Fluorescent immunolabel was visualized with a Leica confocal laser scanning microscope.

Immunoblotting. Confluent 3T3-L1 fibroblasts and 3T3-L1 adipocytes at day 8 of differentiation were serum starved for 2 h and lysed in phosphate-buffered saline containing 1% Triton X-100, 1 mM EDTA, 1 mM phenylmethylsulfonyl fluoride, 10 μg of aprotinin per ml, and 10 μg of leupeptin per ml. Equal amounts of protein were subjected to sodium dodecyl sulfate-polyacrylamide gel electrophoresis (SDS-PAGE) and transferred to a polyvinylidene difluoride membrane. Membranes were incubated with the indicated antibodies. Horseradish peroxidase-conjugated secondary antibodies were visualized with ECL reagent (Pierce, Rockford, Ill.) and a 16-bit camera-based imager (VersaDoc 5000; Bio-Rad, Regents Park, Australia). For quantitation, a serial dilution of a control sample was run on the same SDS-PAGE gel, and Quantity One software (Bio-Rad) was used for analysis. An anti-HA immunoblot was used to determine the relative expression of GLUT4 Tail, as this GLUT4 molecule was not recognized by the anti-GLUT4 antibody.

RESULTS

A novel assay was developed to analyze the intracellular trafficking of GLUT4. This assay was based on the retroviral expression of GLUT4 with an HA epitope tag in its first exofacial loop (21). To characterize the trafficking itinerary of GLUT4 in detail, three GLUT4 mutants were included in the studies described here: GLUT4 Tail, GLUT4 L489,490A, and GLUT4 F5A (Fig. 1A). The GLUT4 Tail mutant, in which the C-terminal 12 amino acid residues are replaced by the corresponding residues of GLUT3, is defective in transport between endosomes and the syntaxin 16-positive perinuclear compartment (28). Unlike wild-type GLUT4, this mutant is mainly localized in endosomes. This localization pattern is induced by the absence of the 12 residues of GLUT4, as the presence of the 12 C-terminal residues of GLUT3 does not affect GLUT4 trafficking (17, 27).

The Leu-489,490 and Phe-5 motifs play a role in GLUT4 endocytosis. The retrovirus-based expression of these mole-

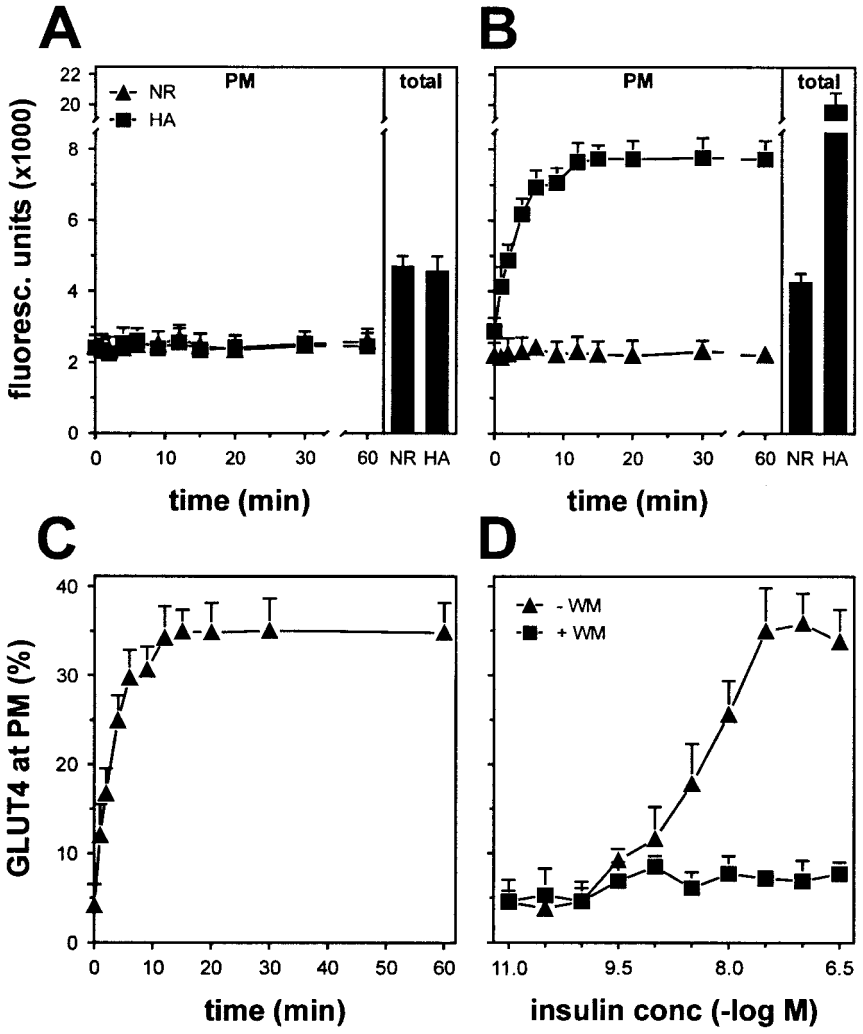

FIG. 2. Analysis of insulin-induced GLUT4 translocation with a novel assay. Noninfected (A) or HA-GLUT4-expressing 3T3-L1 adipocytes (B) were grown in 96-well plates and stimulated for the indicated periods with 200 nM insulin. After fixation, cells were incubated with or without saponin to allow the labeling of all cellular GLUT4 (total) and PM-localized GLUT4 (PM), respectively. Subsequently, cells were incubated with nonrelevant (NR) or anti-HA (HA) antibody and with Alexa 488-conjugated goat anti-mouse antibody, after which fluorescence was measured with a fluorescence plate reader. (C) With the fluorescence values from panel B, anti-HA-specific labeling at the plasma membrane was expressed as percentage of total anti-HA-specific labeling. (D) 3T3-L1 adipocytes were incubated for 20 min with insulin as indicated, in the absence or presence of 100 nM wortmannin, and analyzed as described for panel C. Representative experiments are shown.

cules allowed detailed quantitative analysis because most cells (≈90%) expressed the reporter molecule (Fig. 1B). Furthermore, there was a modest level of overexpression (Fig. 1C and D), making it unlikely that GLUT4 localization was disturbed due to saturation of the cellular trafficking machinery. Steady-state labeling of unstimulated cells revealed a predominant perinuclear GLUT4 localization in fibroblasts with low levels of GLUT4 in small peripheral vesicles. GLUT4 Tail was more concentrated in peripheral vesicles than wild-type GLUT4 when expressed in fibroblasts (Fig. 1E). This localization pattern was induced by the absence of the acidic targeting motif ^{499}EXEY^{502} (data not shown) and is in agreement with our earlier findings that implicate these residues in the exit of GLUT4 from an endosomal compartment (28). All GLUT4 molecules displayed a similar localization pattern in adipocytes, mostly perinuclear and in numerous vesicles throughout the cytoplasm.

Novel assay to study GLUT4 trafficking. To determine the extent of insulin-induced GLUT4 translocation with the assay described here, HA-GLUT4-expressing 3T3-L1 adipocytes grown in 96-well plates were incubated for 2 h in the absence of serum, after which 200 nM insulin was added at various time points and the cell surface levels of HA-GLUT4 were analyzed by indirect immunofluorescence labeling (Fig. 2B). Saturating amounts of anti-HA and secondary antibodies were used to ensure that all HA-GLUT4 molecules were labeled. A nonrelevant antibody was used at the same concentration to determine the nonspecific binding of the anti-HA antibody. Insulin stimulated the appearance of HA-GLUT4 at the PM with a half-time of about 2.5 min, reaching a plateau by 12 min which

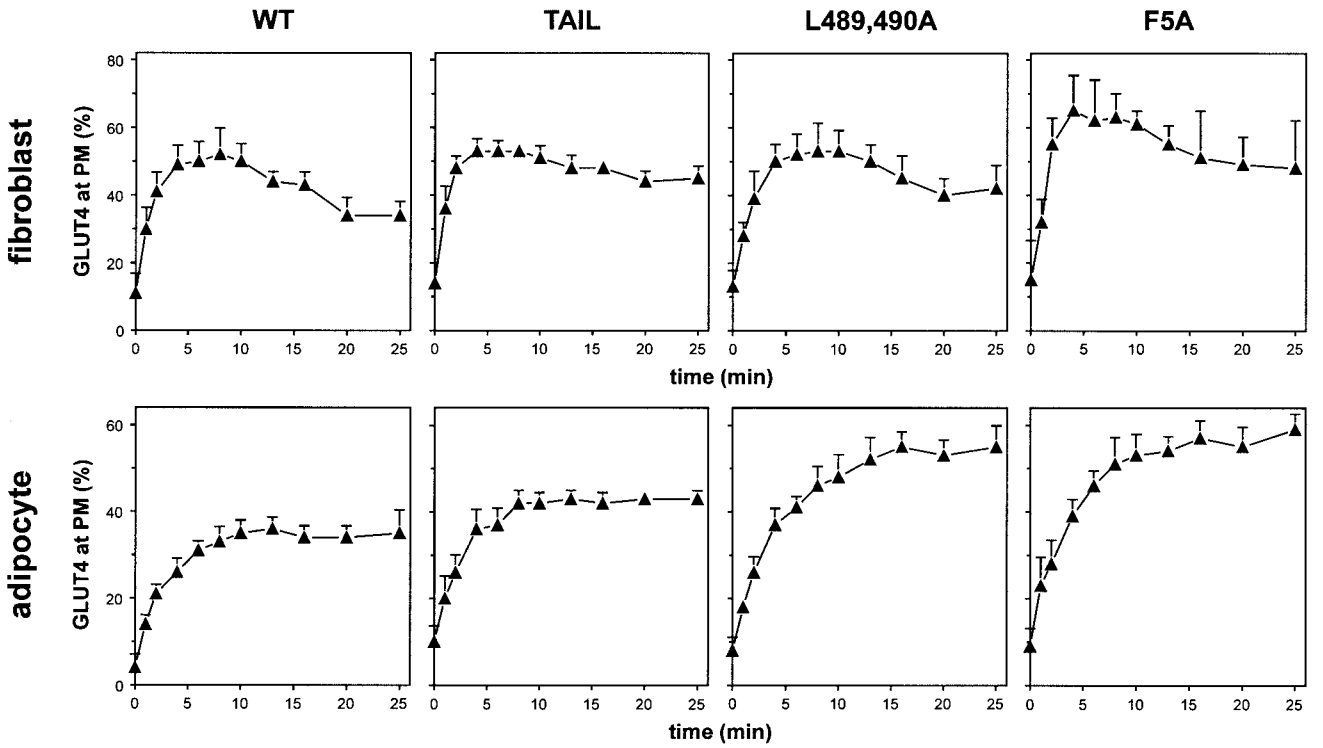

FIG. 3. Insulin-induced GLUT4 translocation in 3T3-L1 fibroblasts and adipocytes. Fibroblasts and adipocytes expressing the indicated GLUT4 molecules were incubated with 200 nM insulin for up to 25 min, and the percentage of GLUT4 at the PM was determined as in Fig. 2.

was maintained for at least 60 min. No specific anti-HA labeling was detected in noninfected cells (Fig. 2A). Expressing the amount of specific fluorescence at the PM as a percentage of the total specific fluorescence revealed that insulin increased the amount of GLUT4 at the PM from a basal value of 4% up to 34% (Fig. 2C), and this effect was inhibited by wortmannin (Fig. 2D).

Insulin-induced GLUT4 translocation in 3T3-L1 fibroblasts and adipocytes. Insulin induced the translocation of wild-type GLUT4 and each of the GLUT4 mutants to the PM in 3T3-L1 fibroblasts (Fig. 3). The maximum level of surface GLUT4 was reached after 6 min of insulin stimulation, representing a five-fold increase above that observed in nonstimulated cells, followed by a rapid reduction. The PM level of the GLUT4 F5A mutant was slightly higher than that of the other GLUT4 molecules in insulin-stimulated fibroblasts. In adipocytes, we observed a ≈8-fold increase in cell surface GLUT4 levels in response to insulin stimulation. Neither wild-type GLUT4 nor any of the GLUT4 mutants showed an overshoot, as was observed in fibroblasts. The GLUT4 Tail mutant showed translocation characteristics similar to those of wild-type GLUT4, although cell surface levels in both the absence and presence of insulin were increased by approximately 5%, in accordance with previous studies (27). The PM levels of both the L489,490A and F5A mutants were significantly higher than those of wild-type GLUT4 in both the absence and presence of insulin. The insulin-induced translocation of wild-type GLUT4 and GLUT4 Tail in fibroblasts and adipocytes was further confirmed by immunofluorescence labeling (see Fig. S1 in the supplemental material).

Analysis of GLUT4 internalization in 3T3-L1 adipocytes. Wild-type GLUT4 molecules that were labeled with anti-HA antibody on ice were rapidly cleared from the cell surface, as indicated by the disappearance of GLUT4 at early time points after transfer of the cells from ice to 37°C (Fig. 4). After approximately 5 min, the amount of GLUT4 at the PM reached steady state in the presence but not in the absence of insulin, consistent with recycling of GLUT4 back to the PM in insulin-stimulated cells. Our data indicated that after 2 min at 37°C, ≈50% of both wild-type GLUT4 and GLUT4 Tail had disappeared from the PM. Importantly, this internalization rate was unaffected by insulin, consistent with previous studies (25). The internalization rates for the L489,490A and F5A mutants were decreased by 30 and 45%, respectively.

Anti-HA antibody uptake by HA-GLUT4-expressing 3T3-L1 fibroblasts and adipocytes. To analyze the exchange of GLUT4 with the cell surface under steady-state conditions, studies were performed in which live cells were incubated with anti-HA antibody at 37°C (Fig. 5). To ascertain that the anti-HA antibody did not affect the intracellular trafficking of HA-GLUT4, control experiments were performed in which insulin-induced translocation of anti-HA-bound HA-GLUT4 was studied. 3T3-L1 adipocytes expressing HA-tagged wild-type GLUT4 were stimulated for 2 h with 200 nM insulin in the presence of anti-HA antibody, washed extensively, incubated for 2 h without insulin and anti-HA, and incubated for a fur-

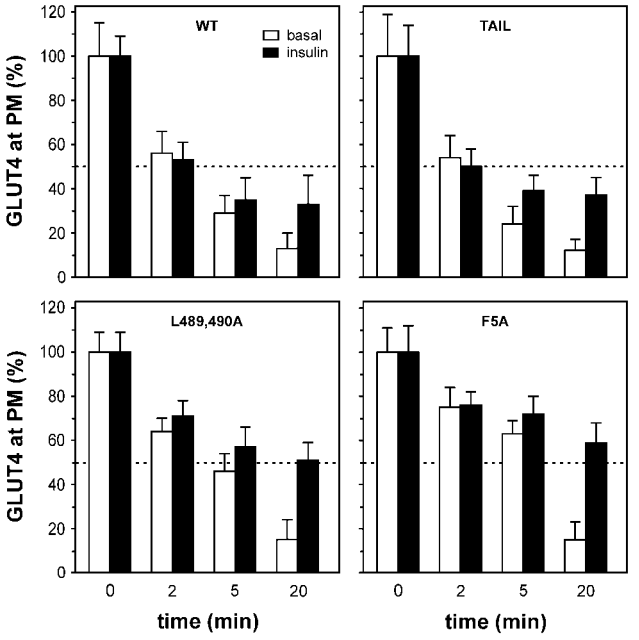

FIG. 4. Internalization kinetics of GLUT4 in 3T3-L1 adipocytes. Adipocytes expressing the indicated GLUT4 molecules were incubated for 20 min with 200 nM insulin at 37°C and for 1 h with anti-HA antibody on ice. Excess antibody was washed away, and cells were incubated for the indicated periods at 37°C in the presence of either 100 nM wortmannin, to measure GLUT4 internalization in the basal state, or 200 nM insulin. Cells were exposed to fixative and incubated with fluorescent secondary antibody in the absence of permeabilizing agent to allow measurement of the time-dependent disappearance of anti-HA-labeled GLUT4 from the cell surface.

ther 20 min in the absence (Fig. 5C) or presence (Fig. 5D) of 200 nM insulin. The cells showed insulin-induced redistribution of anti-HA-bound HA-GLUT4 from intracellular compartments to the PM that was indistinguishable from the translocation of HA-GLUT4 that had not been labeled with antibody (Fig. 5A and B), indicating that the anti-HA antibody had no significant effect on GLUT4 trafficking.

For quantification of anti-HA antibody uptake, cells were incubated for 20 min in the presence or absence of insulin, after which anti-HA antibody or control antibody was added for various times in the continued presence or absence of insulin (Fig. 5E). Antibody uptake was determined by labeling cells after fixation with a fluorescent secondary antibody and was expressed as a percentage of postfixation anti-HA labeling of permeabilized cells. Several novel observations were made from these studies. First, there was a profound difference in recycling kinetics for HA-GLUT4 between fibroblasts and adipocytes in the absence of insulin. Whereas a significant portion of the GLUT4 molecules recycled between intracellular compartments and the PM in nonstimulated fibroblasts (≈50% after 60 min), this was not the case in adipocytes, with only ≈10% of the entire GLUT4 pool labeled after 3 h. Recycling of HA-GLUT4 in the presence of insulin was similar for fibroblasts and adipocytes. Second, the recycling rate of HA-GLUT4 Tail in nonstimulated adipocytes was significantly higher than that observed for wild-type GLUT4. Third, both of the internalization mutants showed a minor increase in basal anti-HA uptake and no difference in uptake during insulin stimulation compared with wild-type GLUT4. Finally, it was noted that even with maximum insulin stimulation, a small but significant pool of GLUT4 could not be labeled with antibody at the PM. Control experiments indicated that this was not due to our technique but implied that this GLUT4 pool simply did not exchange with the cell surface under steady-state conditions (see Fig. S2 in the supplemental material). The size of this pool was similar for fibroblasts and adipocytes and for the different GLUT4 mutants. Altogether, the results suggested the presence of an intracellular pool of GLUT4 that was segregated from the insulin-responsive pool.

The recycling kinetics of HA-GLUT4 was studied throughout the adipocyte differentiation process (Fig. 6). In parallel, antibody uptake was analyzed by immunofluorescence confocal microscopy (Fig. 6, left panels) as well as endogenous GLUT4 labeling and lipid droplet content in noninfected cells (Fig. 6, right panels). There was a progressive decline in antibody uptake between days 0 and 4 of differentiation. Expression of endogenous GLUT4 and lipid droplet formation were initially detected at day 3, when antibody uptake by nonstimulated cells had already decreased by 85% (compared with 100% at day 4). The final reduction in basal anti-HA uptake, between days 3 and 4, coincided with a massive growth of the cells (Fig. 6, bottom right panels).

Insulin releases GLUT4 into a cell surface recycling pathway. The extremely small amount of GLUT4 that cycles to the cell surface in nonstimulated adipocytes suggests that we are not dealing with a simple two-compartment system comprised of endosomes and the PM, raising the possibility that our data may be more consistent with a model in which insulin induces the release of GLUT4 from an intracellular storage compartment. This suggests that at submaximal insulin doses, only part of the intracellular GLUT4 pool may be released into a cell surface recycling system, as opposed to reduced trafficking kinetics of the entire intracellular GLUT4 pool.

To test this, we performed recycling studies with different doses of insulin (Fig. 7). These studies revealed that the size of the recycling pool of GLUT4 was incrementally increased with increasing doses of insulin. We observed similar results when the cells were incubated with higher concentrations of anti-HA antibody (not shown). It is highly unlikely that this incremental effect simply reflected a slow time course of exchange of GLUT4 with the recycling system at low insulin doses, as the cells had been incubated with antibody for sufficient time to label these pools to equilibrium (Fig. 7). This phenomenon was evident for both wild-type GLUT4 and GLUT4 Tail, although insulin had a less profound effect on GLUT4 Tail due to its elevated levels in the recycling pathway in the basal state. Measurement of cell surface levels of HA-GLUT4 at the different insulin doses revealed that the insulin dose-response curves for translocation of both wild-type GLUT4 and GLUT4 Tail were identical despite major differences in their basal recycling properties (Fig. 7B).

To rule out the possibility that this incremental effect of insulin on the entry of GLUT4 into a cell surface recycling system might reflect intrinsic differences in insulin sensitivity between individual cells within the culture, we next examined the dose-response relationship in antibody uptake in individual cells by immunofluorescence microscopy. As indicated in Fig.

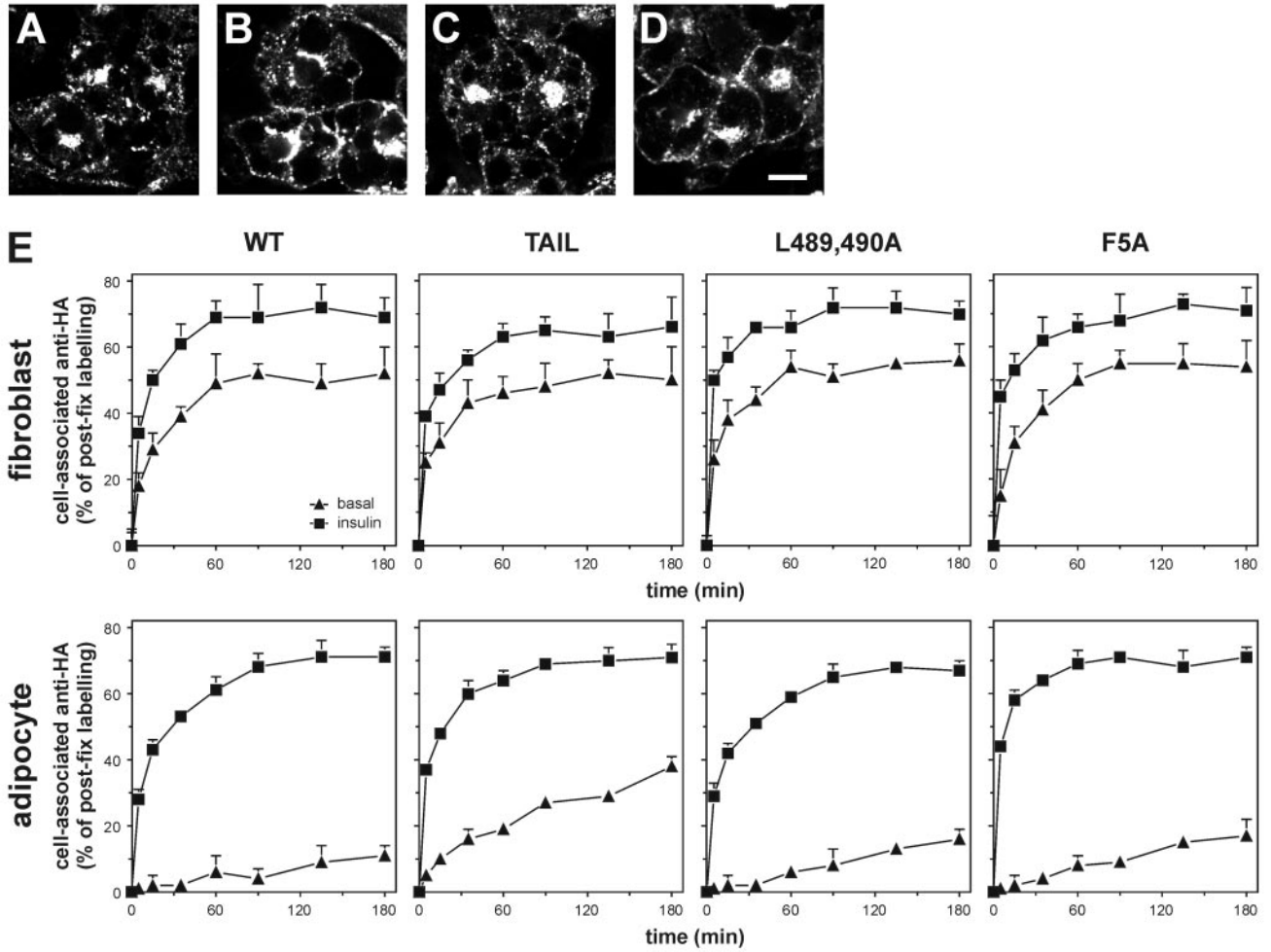

FIG. 5. GLUT4 recycling in 3T3-L1 fibroblasts and adipocytes. HA-GLUT4-expressing adipocytes were incubated for 2 h with 200 nM insulin and subsequently for 2 h without insulin and for 20 min in the absence (A) or presence (B) of 200 nM insulin. Parallel cultures were incubated for 2 h with 200 nM insulin and anti-HA antibody, followed by a 2-h incubation without insulin and anti-HA and a 20-min incubation in the absence (C) or presence (D) of 200 nM insulin. HA-GLUT4 (A and B) and anti-HA antibody (C and D) were visualized by immunolabeling and confocal microscopy. Bar, 10 μm. (E) For quantitation of antibody uptake, fibroblasts and adipocytes expressing the indicated HA-GLUT4 molecules were incubated with or without 200 nM insulin for 20 min, after which anti-HA antibody was added. Cells were incubated further for up to 180 min, fixed, permeabilized, and incubated with fluorescent secondary antibody. The amount of anti-HA antibody taken up by the cells was expressed as a percentage of total postfixation anti-HA labeling.

7C the response among different cells was highly homogeneous, such that at low doses of insulin, most cells exhibited a low level of antibody uptake, and at higher doses, there was a uniform rather than a heterogeneous increase in antibody uptake.

DISCUSSION

In the present study, we describe a novel assay for studying GLUT4 trafficking. This assay recapitulates many of the known facets of insulin-responsive GLUT4 trafficking, including a major effect of insulin on exocytosis with little if any effect on GLUT4 endocytosis. In addition, we made several novel observations that provide new insight into the relationship between insulin action and endosomal trafficking. First, adipocytes possess a highly efficient intracellular GLUT4 sequestration mechanism that does not operate efficiently in preadipocytes (Fig. 5). This mechanism is sufficiently robust that the majority of the intracellular GLUT4 pool does not exchange with the PM in the absence of insulin. This suggests that the recycling pool and the insulin-regulated pool operate in a mutually exclusive manner under these conditions. The entry of GLUT4 into the sequestered pool involves the acidic targeting signal located within the cytosolic C terminus of GLUT4, as disruption of this motif increases the amount of GLUT4 in the PM recycling pathway under basal conditions. Second, insulin induces the release of GLUT4 into a cell surface recycling system in a graded insulin dose-dependent manner. At low insulin doses, 10 to 20% of the entire GLUT4 pool entered the cell surface recycling pathway, and at maximal insulin doses, this was increased to 70%. Hence, this is consistent with a model in which insulin induces the release of GLUT4 into a cell surface recycling pathway in an incremental dose-dependent manner. Third, despite a role for the 12 C-

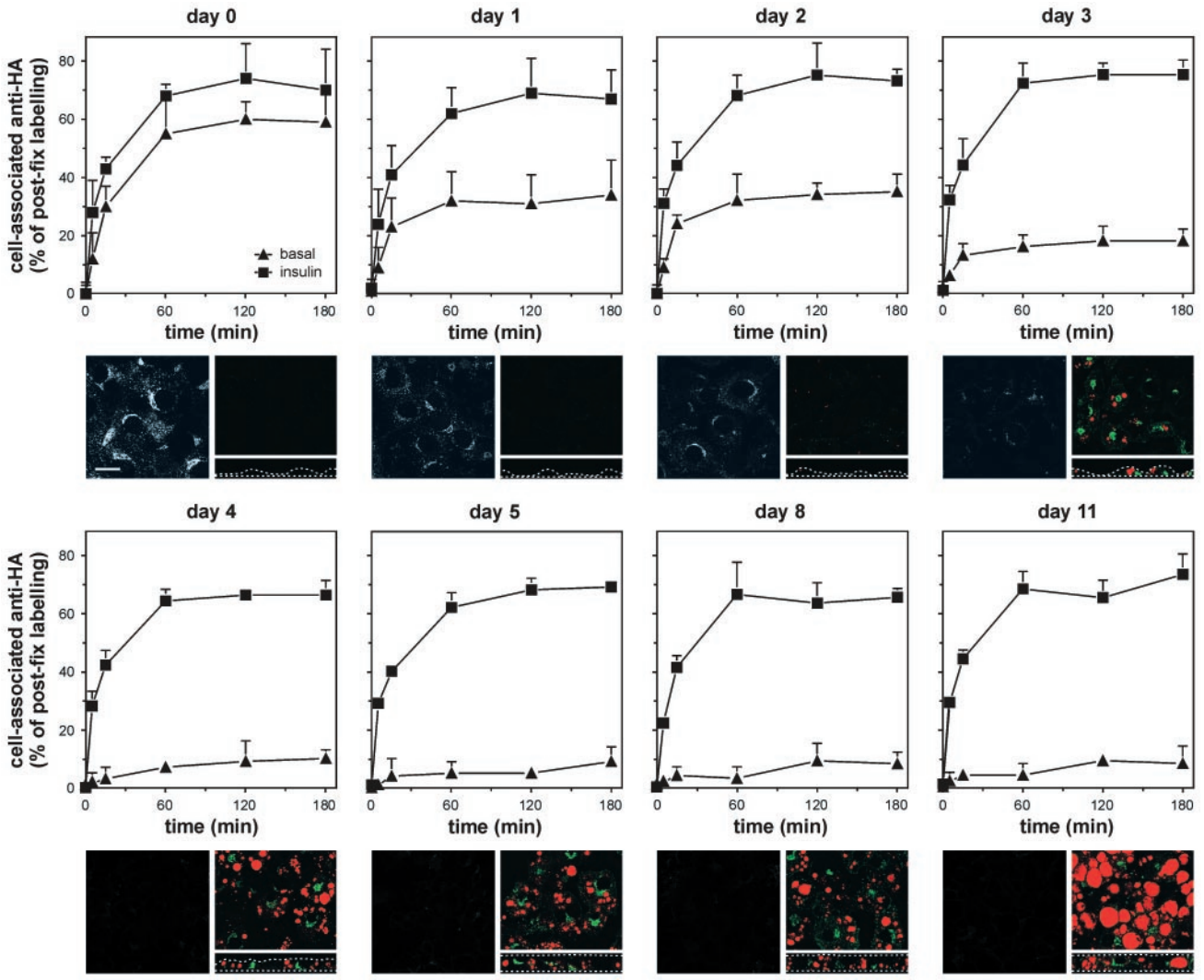

FIG. 6. Analysis of GLUT4 recycling during the differentiation of 3T3-L1 fibroblasts into adipocytes. Cells were analyzed at different stages during differentiation as indicated. After incubation for 18 h in medium containing fetal bovine serum and for 2 h in the absence of serum, the cells were incubated in the continuous presence of anti-HA antibody as described for Fig. 5. Parallel cultures were incubated similarly but analyzed by immunofluorescence confocal microscopy (left microscopy panels). Noninfected cells were analyzed for endogenous GLUT4 (green) and lipid droplet content (red) during differentiation (right microscopy panels). The bottom right microscopy panels show a Z-section image of the cells. White dotted lines mark the contours of the cells. Bar, 20 μm.

terminal residues and the ^{5}FQQI^{8} and ^{489}LL^{490} motifs in several aspects of GLUT4 trafficking, the main domain(s) within GLUT4 that is involved in its acute insulin-induced cell surface translocation remains to be established.

Intracellular sequestration of GLUT4. A striking observation made in this study is that in the absence of insulin, little of the intracellular GLUT4 pool is in communication with the cell surface under steady-state conditions. These data suggest that a large pool must be stored or sequestered in such a way that it never enters the recycling system. Otherwise we would have expected a slow but continuous increase in the amount of GLUT4 molecules that would be labeled with antibody. What is the nature of this intracellular GLUT4 compartment? We have previously shown that GLUT4 labeled at the cell surface rapidly transits through endosomes to a perinuclear compartment that also contains syntaxin 16 (28). It is likely that this endosome-TGN cycle plays an important role in the intracellular sequestration of GLUT4, because we show in the present study that, in adipocytes, a GLUT4 mutant that is defective in this endosome-TGN transport cycle (GLUT4 Tail) displays an increased amount of GLUT4 in the cell surface recycling pathway in the absence of insulin (Fig. 5). Moreover, when expressed in 3T3-L1 fibroblasts, ≈50% of GLUT4 enters the surface recycling system in the absence of insulin, while these cells show little overlap between GLUT4 and syntaxin 16 (data not shown). Collectively, these data suggest that GLUT4 is selectively transported from endosomes to a subdomain of the TGN that contains syntaxin 16. This pathway is elaborated upon adipocyte differentiation and plays a role in maintaining low surface levels of GLUT4 in the absence of insulin. This is consistent with previous modeling studies that show that, in 3T3-L1 fibroblasts, GLUT4 trafficking can be explained by a

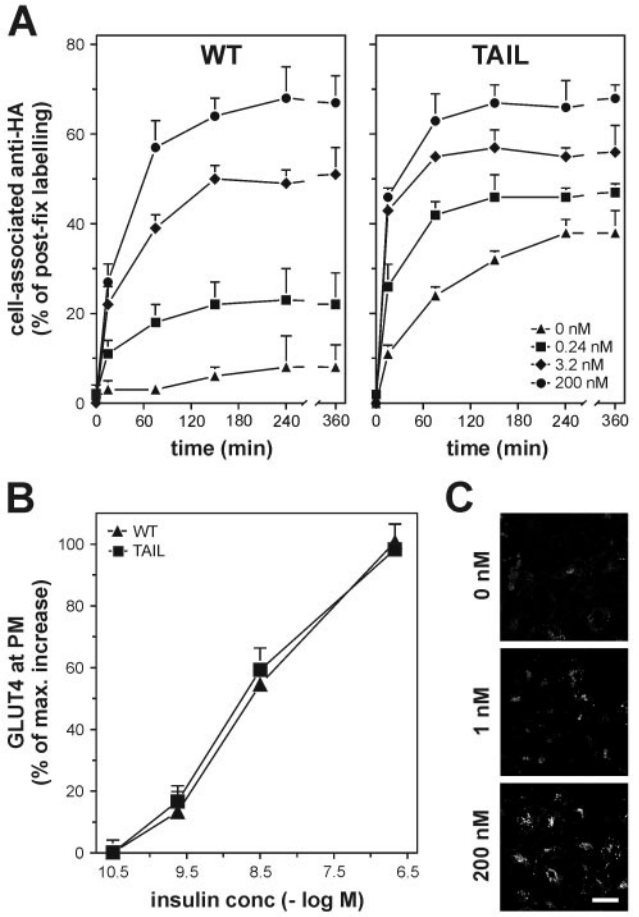

FIG. 7. Correlation between insulin concentration and the size of the recycling GLUT4 pool in 3T3-L1 adipocytes. (A) 3T3-L1 adipocytes expressing HA-tagged wild-type GLUT4 and HA-GLUT4 Tail were incubated at 37°C with anti-HA antibody and the indicated concentrations of insulin and analyzed as described. (B) 3T3-L1 adipocytes expressing HA-tagged wild-type GLUT4 and GLUT4 Tail were incubated for 20 min at 37°C with 0.032, 0.24, 3.2, or 200 nM insulin, and the amounts of GLUT4 at the PM were determined and expressed as a percentage of maximal insulin-induced GLUT4 translocation. (C) HA-GLUT4-expressing 3T3-L1 adipocytes were incubated for 3 h with anti-HA antibody and the indicated concentrations of insulin. Cells were fixed, permeabilized, incubated with fluorescent secondary antibody, and analyzed by confocal immunofluorescence microscopy. Bar, 20 μm.

two-compartment model in which GLUT4 is slowly recycled to the PM, whereas in 3T3-L1 adipocytes, GLUT4 trafficking is best described by a model composed of three compartments (34).

This transition is clearly seen in Fig. 6, where we examined the recycling kinetics of GLUT4 at different stages during 3T3-L1 adipocyte differentiation. In agreement with previous studies by El-Jack and colleagues (6), we observed a progressive reduction in basal GLUT4 recycling that was most efficient at day 4 of differentiation. This time course paralleled the increase in endogenous GLUT4 expression that occurred during differentiation. Based on our findings, we suggest that an important component of this transition is the development of the endosome-to-TGN trafficking pathway. It is unlikely, however, that this pathway alone accounts for the very low amount of GLUT4 in the cell surface recycling pathway in nonstimulated adipocytes because the amount of GLUT4 Tail found in this pathway is much less than that observed in nonstimulated fibroblasts, while in both cell types Tail is not present in the TGN. The nature of this additional sorting mechanism remains to be established but may involve partitioning of wild-type GLUT4 and GLUT4 Tail into a second insulin-responsive storage compartment. As GLUT4 Tail is localized in endosomes (28) yet displays a robust insulin-induced translocation, the second retention mechanism may be present within endosomes. Further study is required to resolve this question. In accordance, other studies have suggested an endosomal GLUT4 retention mechanism (13, 35). Possibly, the recently discovered GLUT4 tethering protein TUG plays a role in this process (2).

It is noteworthy that a recent study reported that the basal recycling rate of GLUT4 in adipocytes was not as slow as that reported in the present study and that eventually the entire pool of GLUT4 equilibrated with the PM, with a half time of 4 h (12). We attempted to establish the basis for the difference between the two studies, but so far we have not pinpointed the reason for this controversy. However, in contrast to the present study, McGraw and colleagues used a transient expression system involving electroporation to introduce the relevant reporter into the mature adipocyte and used a single-cell immunofluorescence-based assay to quantify trafficking kinetics. Regardless, both studies indicate that, in basal adipocytes, GLUT4 is recycling very slowly, emphasizing the importance of establishing the nature of the intracellular storage compartment.

Insulin-stimulated GLUT4 translocation. The exceedingly small amount of GLUT4 that recycles to the PM in basal adipocytes raises the intriguing possibility that insulin regulates GLUT4 trafficking via a secretory or release mechanism rather than by mobilizing the entire intracellular pool at discrete kinetic rates. Perhaps the most definitive proof of this mechanism was the demonstration that, at different doses of insulin, there was a progressive increase in the total amount of GLUT4 introduced into the cell surface recycling pathway rather than simply a change in the rate of movement of a defined GLUT4 pool (Fig. 7A). A similar mechanism was also observed for GLUT4 Tail, although the magnitude of this response was restricted by the elevated basal recycling. In support of our data, in 3T3-L1 adipocytes insulin increases the amount of GLUT4-containing vesicles moving along microtubules rather than increasing the speed of vesicle movement (26). This may reflect insulin-induced enhancement of the interaction between the motor protein kinesin, known to play a role in GLUT4 trafficking, and microtubules (9).

These observations are quite novel and raise a series of questions concerning the mechanism of GLUT4 translocation. Most importantly, where is GLUT4 recruited from in response to insulin? It is unlikely that the TGN (sub)compartment alone contributes to this response because GLUT4 Tail is excluded from this trafficking pathway yet retains a robust acute insulin response in adipocytes. Similarly, in 3T3-L1 fibroblasts, where the endosome-TGN cycle does not appear to play a dominant role in GLUT4 trafficking, we (Fig. 3) and others (3, 13) have observed robust insulin-dependent movement of GLUT4 to

the PM. However, it has also been reported that 3T3-L1 fibroblasts are not insulin responsive (8, 24). There are several explanations for this controversy. First, 3T3-L1 fibroblasts become more insulin responsive upon reaching confluence (32). In preconfluent and confluent 3T3-L1 fibroblasts, insulin increases the cell surface levels of GLUT4 by 70 and 270%, respectively (13, 35). In accordance, we used confluent fibroblasts throughout our studies. Second, the overshoot phenomenon originally described by Bogan and colleagues (3) and shown in Fig. 3 implies that many investigators may have overlooked the transient peak in cell surface GLUT4 levels after insulin stimulation, as most studies rely on single-endpoint measurements. Regardless, not all cells seem to exhibit an insulin-responsive GLUT4 translocation system, as exemplified by recent experiments in C2C12 cells (31).

Another reason to believe that the TGN (sub)compartment is unlikely to be the sole contributor of insulin-responsive GLUT4 is that quantitative immunoelectron microscopy has indicated that insulin causes a major decrease in GLUT4 labeling in adipocytes in a population of cytosolic vesicles rather than in the perinuclear compartment (20, 23). These vesicles appeared to be devoid of a variety of markers for generic compartments, suggesting that they represent a unique population of secretory membranes. The question is whether these vesicles are the sole determinant of the insulin-stimulated translocation pathway or whether there multiple insulin-dependent routes to the cell surface. We are currently trying to address this question by studying the trafficking of GLUT4 Tail in adipocytes and that of GLUT4 in fibroblasts. Intriguingly, in CHO cells, GLUT4 and transferrin receptor are packaged into separate vesicles en route to the PM (14), suggesting that these unique secretory vesicles may exist in fibroblasts.

Intriguingly, we observed that not all of the cellular GLUT4 (≈30%) participates in insulin-induced trafficking to the cell surface. Of note, the size of this pool was similar for GLUT4 and GLUT4 Tail in adipocytes as well as for GLUT4 when expressed in fibroblasts (Fig. 5). Thus, it is tempting to speculate that this pool may be related to the insulin-responsive compartment, as this is common to both of these situations. A similar phenomenon has been described for the asialoglycoprotein receptor, whereby only 70% could be labeled with ligand under steady-state conditions (30). One possibility is that these latent pools may be related to the age of the molecules in the cell. It has recently been shown that younger populations of secretory granules in neuroendocrine cells are preferentially secreted in response to stimulation compared to older granules (5). Perhaps GLUT4 that is present in the latent pool represents molecules that were synthesized early in the life of the cell, whereas newer molecules may preferentially undergo insulin-dependent exocytosis. If GLUT4 is distributed in this manner, it is fortuitous that we used a system in which the HA-GLUT4 reporter was present in the 3T3-L1 cells for more than 10 days, allowing it to equilibrate with endogenous GLUT4 within this latent pool.

In summary, the present study demonstrates that the constitutive trafficking of GLUT4 to the PM is largely reduced during the differentiation of 3T3-L1 fibroblasts into adipocytes. In adipocytes, insulin causes a dose-dependent release of GLUT4 into the recycling pathway, leading to dose-dependent increases in cell surface GLUT4 levels. The released GLUT4 molecules do not mix with the non-insulin-responsive GLUT4 pool during recycling, indicating the existence of distinct, slowly communicating pools of GLUT4 within the adipocyte. A major aim will now be to dissect the intracellular GLUT4 sequestration machinery. Unraveling this machinery will bring us closer to an understanding of insulin action and to the management of type 2 diabetes.

ACKNOWLEDGMENTS

We are grateful to Jan-Willem Slot for critical reading of the manuscript and Annette Shewan and Ellen van Dam for generation of retrovirus.

This work was supported by a fellowship from the European Molecular Biology Organization (to R.G.) and grants from the National Health and Medical Research Council of Australia and Diabetes Australia (to D.E.J.).

REFERENCES

1. **Al-Hasani, H., C. S. Hinck, and S. W. Cushman.** 1998. Endocytosis of the glucose transporter GLUT4 is mediated by the GTPase dynamin. J. Biol. Chem. **273:**17504–17510.
2. **Bogan, J. S., N. Hendon, A. E. McKee, T. S. Tsao, and H. F. Lodish.** 2003. Functional cloning of TUG as a regulator of GLUT4 glucose transporter trafficking. Nature **425:**727–733.
3. **Bogan, J. S., A. E. McKee, and H. F. Lodish.** 2001. Insulin-responsive compartments containing GLUT4 in 3T3-L1 and CHO cells: regulation by amino acid concentrations. Mol. Cell. Biol. **21:**4785–4806.
4. **Bryant, N. J., R. Govers, and D. E. James.** 2002. Regulated transport of the glucose transporter GLUT4. Nat. Rev. Mol. Cell. Biol. **3:**267–277.
5. **Duncan, R. R., J. Greaves, U. K. Wiegand, I. Matskevich, G. Bodammer, D. K. Apps, M. J. Shipston, and R. H. Chow.** 2003. Functional and spatial segregation of secretory vesicle pools according to vesicle age. Nature **422:** 176–180.
6. **El-Jack, A. K., K. V. Kandror, and P. F. Pilch.** 1999. The formation of an insulin-responsive vesicular cargo compartment is an early event in 3T3-L1 adipocyte differentiation. Mol. Biol. Cell **10:**1581–1594.
7. **Gillingham, A. K., F. Koumanov, P. R. Pryor, B. J. Reaves, and G. D. Holman.** 1999. Association of AP1 adaptor complexes with GLUT4 vesicles. J. Cell Sci. **112:**4793–4800.
8. **Haney, P. M., J. W. Slot, R. C. Piper, D. E. James, and M. Mueckler.** 1991. Intracellular targeting of the insulin-regulatable glucose transporter (GLUT4) is isoform specific and independent of cell type. J. Cell Biol. **114:**689–699.
9. **Imamura, T., J. Huang, I. Usui, H. Satoh, J. Bever, and J. M. Olefsky.** 2003. Insulin-induced GLUT4 translocation involves protein kinase C-lambda-mediated functional coupling between Rab4 and the motor protein kinesin. Mol. Cell. Biol. **23:**4892–4900.
10. **Johnson, A. O., M. A. Lampson, and T. E. McGraw.** 2001. A di-leucine sequence and a cluster of acidic amino acids are required for dynamic retention in the endosomal recycling compartment of fibroblasts. Mol. Biol. Cell **12:**367–381.
11. **Johnson, A. O., A. Subtil, R. Petrush, K. Kobylarz, S. R. Keller, and T. E. McGraw.** 1998. Identification of an insulin-responsive, slow endocytic recycling mechanism in Chinese hamster ovary cells. J. Biol. Chem. **273:**17968–17977.
12. **Karylowski, O., A. Zeigerer, A. Cohen, and T. E. McGraw.** 2004. GLUT4 is retained by an intracellular cycle of vesicle formation and fusion with endosomes. Mol. Biol. Cell **15:**870–882.
13. **Lampson, M. A., A. Racz, S. W. Cushman, and T. E. McGraw.** 2000. Demonstration of insulin-responsive trafficking of GLUT4 and vpTR in fibroblasts. J. Cell Sci. **113:**4065–4076.
14. **Lampson, M. A., J. Schmoranzer, A. Zeigerer, S. M. Simon, and T. E. McGraw.** 2001. Insulin-regulated release from the endosomal recycling compartment is regulated by budding of specialized vesicles. Mol. Biol. Cell **12:**3489–3501.
15. **Livingstone, C., D. E. James, J. E. Rice, D. Hanpeter, and G. W. Gould.** 1996. Compartment ablation analysis of the insulin-responsive glucose transporter (GLUT4) in 3T3-L1 adipocytes. Biochem. J. **315:**487–495.
16. **Malide, D., and S. W. Cushman.** 1997. Morphological effects of wortmannin on the endosomal system and GLUT4-containing compartments in rat adipose cells. J. Cell Sci. **110:**2795–2806.
17. **Marsh, B. J., R. A. Alm, S. R. McIntosh, and D. E. James.** 1995. Molecular regulation of GLUT-4 targeting in 3T3-L1 adipocytes. J. Cell Biol. **130:**1081–1091.
18. **Martin, S., G. Ramm, C. T. Lyttle, T. Meerloo, W. Stoorvogel, and D. E. James.** 2000. Biogenesis of insulin-responsive GLUT4 vesicles is independent of brefeldin A-sensitive trafficking. Traffic **1:**652–660.

19. **Martin, S., B. Reaves, G. Banting, and G. W. Gould.** 1994. Analysis of the colocalization of the insulin-responsive glucose transporter (GLUT4) and the trans Golgi network marker TGN38 within 3T3-L1 adipocytes. Biochem. J. **300:**743–749.
20. **Martin, S., J. Tellam, C. Livingstone, J. W. Slot, G. W. Gould, and D. E. James.** 1996. The glucose transporter (GLUT-4) and vesicle-associated membrane protein-2 (VAMP-2) are segregated from recycling endosomes in insulin-sensitive cells. J. Cell Biol. **134:**625–635.
21. **Quon, M. J., M. Guerre-Millo, M. J. Zarnowski, A. J. Butte, M. Em, S. W. Cushman, and S. I. Taylor.** 1994. Tyrosine kinase-deficient mutant human insulin receptors (Met1153→Ile) overexpressed in transfected rat adipose cells fail to mediate translocation of epitope-tagged GLUT4. Proc. Natl. Acad. Sci. USA **91:**5587–5591.
22. **Ralston, E., and T. Ploug.** 1996. GLUT4 in cultured skeletal myotubes is segregated from the transferrin receptor and stored in vesicles associated with TGN. J. Cell Sci. **109:**2967–2978.
23. **Ramm, G., J. W. Slot, D. E. James, and W. Stoorvogel.** 2000. Insulin recruits GLUT4 from specialized VAMP2-carrying vesicles as well as from the dynamic endosomal/Trans-Golgi network in rat adipocytes. Mol. Biol. Cell **11:**4079–4091.
24. **Ross, S. A., S. R. Keller, and G. E. Lienhard.** 1998. Increased intracellular sequestration of the insulin-regulated aminopeptidase upon differentiation of 3T3-L1 cells. Biochem. J. **330:**1003–1008.
25. **Satoh, S., H. Nishimura, A. E. Clark, I. J. Kozka, S. J. Vannucci, I. A. Simpson, M. J. Quon, S. W. Cushman, and G. D. Holman.** 1993. Use of bismannose photolabel to elucidate insulin-regulated GLUT4 subcellular trafficking kinetics in rat adipose cells. Evidence that exocytosis is a critical site of hormone action. J. Biol. Chem. **268:**17820–17829.
26. **Semiz, S., J. G. Park, S. M. Nicoloro, P. Furcinitti, C. Zhang, A. Chawla, J. Leszyk, and M. P. Czech.** 2003. Conventional kinesin KIF5B mediates insulin-stimulated GLUT4 movements on microtubules. EMBO J. **22:**2387–2399.
27. **Shewan, A. M., B. J. Marsh, D. R. Melvin, S. Martin, G. W. Gould, and D. E. James.** 2000. The cytosolic C-terminus of the glucose transporter GLUT4 contains an acidic cluster endosomal targeting motif distal to the dileucine signal. Biochem. J. **350:**99–107.
28. **Shewan, A. M., E. M. Van Dam, S. Martin, T. B. Luen, W. Hong, N. J. Bryant, and D. E. James.** 2003. GLUT4 Recycles via a trans-Golgi network (TGN) subdomain enriched in syntaxins 6 and 16 but not TGN38: involvement of an acidic targeting motif. Mol. Biol. Cell **14:**973–986.
29. **Slot, J. W., H. J. Geuze, S. Gigengack, G. E. Lienhard, and D. E. James.** 1991. Immuno-localization of the insulin regulatable glucose transporter in brown adipose tissue of the rat. J. Cell Biol. **113:**123–135.
30. **Stoorvogel, W., H. J. Geuze, J. M. Griffith, A. L. Schwartz, and G. J. Strous.** 1989. Relations between the intracellular pathways of the receptors for transferrin, asialoglycoprotein, and mannose 6-phosphate in human hepatoma cells. J. Cell Biol. **108:**2137–2148.
31. **Tortorella, L. L., and P. F. Pilch.** 2002. C2C12 myocytes lack an insulin-responsive vesicular compartment despite dexamethasone-induced GLUT4 expression. Am. J. Physiol. **283:**E514–524.
32. **Yang, J., A. E. Clark, I. J. Kozka, S. W. Cushman, and G. D. Holman.** 1992. Development of an intracellular pool of glucose transporters in 3T3-L1 cells. J. Biol. Chem. **267:**10393–10399.
33. **Yang, J., J. F. Clarke, C. J. Ester, P. W. Young, M. Kasuga, and G. D. Holman.** 1996. Phosphatidylinositol 3-kinase acts at an intracellular membrane site to enhance GLUT4 exocytosis in 3T3-L1 cells. Biochem. J. **313:** 125–131.
34. **Yeh, J. I., K. J. Verhey, and M. J. Birnbaum.** 1995. Kinetic analysis of glucose transporter trafficking in fibroblasts and adipocytes. Biochemistry **34:**15523–15531.
35. **Zeigerer, A., M. A. Lampson, O. Karylowski, D. D. Sabatini, M. Adesnik, M. Ren, and T. E. McGraw.** 2002. GLUT4 retention in adipocytes requires two intracellular insulin-regulated transport steps. Mol. Biol. Cell **13:**2421–2435.